

# **Numerical Classical and Quantum Mechanical simulations of Charge Density Wave models.**

A. W. Beckwith

Department of Physics and Texas Center for Superconductivity and Advanced  
Materials at the University of Houston  
Houston, Texas 77204-5005, USA

## **Abstract**

We first present how to do a computer simulation of Charge Density Waves using a driven harmonic oscillator model by a numerical scheme as initially formulated by Littlewood, and then afterwards use this to present how the dielectric model as presented via this procedure leads to a blow up at the initialization of a threshold field  $E_T$ . We find that this is highly unphysical and this initiated our inquiry as to alternative models. Afterwards, we then investigate how to present this transport problem of CDW quantum mechanically, through a numerical simulation of the massive Schwinger model. We find that this single chain quantum mechanical simulation used to formulate solutions to CDW transport in itself is insufficient for transport of solitons (anti-solitons) through a pinning gap model of CDW. We show that a model Hamiltonian with Peierls condensation energy used to couple adjacent chains (or transverse wave vectors) permits formation of solitons (anti-solitons) which can be used to transport CDW through a potential barrier. This addition of the Peierls condensation energy term is essential for any quantum model of Charge Density Waves to give tunneling behavior as seen via a numerical simulation.

PACS numbers : **03.75.Lm, 71.45.Lr, 71.55.-i, 78.20.Ci, 85.25.Cp**

## 1.

### Introduction

The classical model of Charge Density wave (CDW) transport, as presented by Gruner, is well understood and answers a host of density wave transport questions which need to be addressed if we wish to understand some of the classical electrodynamic phenomena associated with CDW. However, as we will show in our write up, we obtained a very non linear blow up of the calculated dielectric response of  $\text{NbSe}_3$  which indicates that the Gruner model is in need of revision. This lead to investigations of first a single chain- then a multi chain model of CDW based upon the Massive Schwinger equation model with results we will discuss in our article.

We have prior to this paper formed an argument using the integral Bogomil'nyi inequality to present how a soliton-anti soliton (S-S') pair could form<sup>1,2</sup>. Here, we argue that this is equivalent to putting in a so called multi chain interaction term with a constant term in it proportional to the Peierls gap times a cosine term representing interaction of different CDW chains in our massive Schwinger model<sup>3</sup> which is highly unusual since at first glance adding in an additional potential energy term makes the problem look like a Josephon junction problem with no connection to the fate of the false vacuum hypothesis. We found in our investigation that a single chain simulation of the problem suffers from two defects. First, it does not answer what are We have prior to this paper formed an argument using the integral Bogomil'nyi inequality to present how a soliton-anti soliton (S-S') pair could form<sup>1,2</sup>. Here, we argue that this is equivalent to putting in a so called multi chain interaction term with a constant term in it proportional to the Peierls gap times a cosine term representing interaction of different CDW chains in our massive Schwinger model<sup>3</sup> which is highly unusual since at first glance adding in

an additional potential energy term makes the problem look like a Josephson junction problem with no connection to the fate of the false vacuum hypothesis . We found in our investigation that a single chain simulation of the problem suffers from two defects. First, it does not answer what are necessary and sufficient conditions for formation of a soliton( anti soliton) . More importantly, we also find through numerical simulations of the single chain transport model that one needs additional physical conditions to permit barrier penetration. Our numerical simulation of the single chain problem for CDW involving solitons (anti solitons) gave a resonance condition in transport behavior over time, with no barrier tunneling. The argument here we will present is that the false vacuum hypothesis <sup>1,2,4</sup> is a necessary condition for the formation of soliton – anti soliton (S-S') pairs and that the multi chain term we add to a massive Schwinger equation for CDW transport is a sufficiency condition for the explicit formation of a soliton (anti soliton) in our charge density wave transport problem. We initiate the 2<sup>nd</sup> quantum mechanical section of this monograph by a numerical simulation of the single chain model of CDW , then show how addition of the Peierls condensation energy permits a soliton (anti – soliton) to form. Then we present how to numerically simulate a multi chain CDW simulation

## **2. Presenting the classical Washboard potential using Littlewoods random pinning model**

In 1986, Littlewood <sup>5</sup> presented an innovative scheme which incorporates a classical phase pinning model of Fukuyama, Lee, and Rice <sup>6, 7</sup> for the interaction of impurities in a one dimensional setting. We should note that Littlewood's scheme in

numerical form bears striking semblance to the Sine- Gordon equation <sup>8</sup> for evolution of phase values along a one dimensional crystal. The impurity sites are randomly distributed in one dimension, and we have that the phase term  $\phi(x)$  represents the local ‘position’ of a charge density wave which interacts via an interaction potential of  $V_j(x - R_j) \equiv V \cdot \delta(x - R_j)$  which is a short range interaction between the phase  $\phi(x)$  and an impurity site  $R_j$ .  $V$  happens to be a strength of interaction term which we set equal to unity in our simulation, and the randomly chosen position of impurities,  $R_j$ , so happens to be chosen via a random number generator in our simulation, and this selection done in such a way as to avoid bunching about certain fixed numerical quantities in a one dimensional line. This necessitated an ordering insuring  $R_{j+1} > R_j$ . Given this, Littlewood <sup>5</sup> used an overdamped equation of motion as well as dimensionless units in order to give an evolution equation with a first order derivative of phase with respect to time, assuming that phase  $\phi(x)$  responds ‘instantly’ to the effects of an extremely localized interaction of phase with each impurity site given by  $R_j$ . This last assumption permits us to integrate between impurity sites so as to come up with a first order in time evolution equation for the phase  $\phi(x_j) \equiv \phi_j$  where each  $x_j \equiv c \cdot R_j$ . The constant,  $c$ , is the impurity concentration, and assumes that we have a correlation length  $L$  so that we observe  $c \cdot L^d \gg 1$ , i.e. we have weak impurity pinning( here,  $d$  is the dimensionality of the spatial integration). In our model, we set  $d = 1.0$ . The remainder of this section on classical models is to look at the consequences of taking a DFT ( discrete Fourier transform ) of current  $J \approx \langle \dot{\phi} \rangle$  to obtain computed

conductivity and dielectric values due to the evolution of charge density waves along a one dimensional crystal.

Several caveats are in order. First, we had to keep impurity sites from clustering too closely about the origin. . We could not allow them to be too close to each other. Otherwise we obtain wildly divergent computed numerical values for several computed physical quantities, especially, the derivative of phase with respect to time, leading to spurious results for conductivity even when the applied E field is  $< E_{th}$ . In fact, the scheme became so unstable if we had a lot of impurity sites near the origin that the derivative of phase with respect to time would blow up after only several dozen time steps from an initial time. In contrast with this instability, quite stable values of the derivative of phase with respect to time exist so long as the applied field to a quasi one dimensional metal sample (e.g. NbSe<sub>3</sub>) was less than a strength  $V$  and applied electric field  $E$  having their dimensions ‘rescaled’ by variable changes to non dimensional constants. However, it is important to note that equation 2.1 uses a non uniform distribution of impurity sites which is where there is an interaction between phase and ions in a one dimensional setting. However, the  $\Delta\phi_i$  term below represents the interaction between adjacent impurity sites and shows ‘compression’ ( or deformation ) of the CDW ‘phase’, while assuming the impurity sites as given by  $X_i = cR_i$  have a random distribution of  $R_i$  values, while having  $R_i > R_{i-1}$ .

$$\dot{\phi}_i = \Delta^2 \phi_i + \frac{1}{2} E(X_{i+1} - X_i) + V \sin(\theta_i + \phi_i) \quad (2.1)$$

Equation 2.1 is due, in part to setting the acceleration term  $\ddot{\phi}$  in the (uniform spacing for ‘impurities’) ‘sliding condition’ for CDW presented below equal to zero (called ‘deep

damping' due to importance of the  $\frac{1}{\tau} \dot{\phi}$  term) while then, next, randomizing the position of impurity sites which is initially set equally spaced in equation 2. Furthermore, the  $\theta_i$  expression in equation 2.1 is a 'randomized force term ' which varies according to a random generation of numerical values between zero and  $2\pi$  .. Furthermore although the sliding criteria for CDW mentioned in equation 2.2 below assumes no spatial compression (meaning the presence of CDW only, but of no soliton ) , we can specifically show a distinct spatial behavior for the  $\phi$  'phases' as generated by equation 2.1 above. We now refer to the uniform spacing between impurity sites equation for the evolution of phase values, by

$$\ddot{\phi} + \frac{1}{\tau} \dot{\phi} + \omega_0^2 \sin \phi = e \cdot \frac{Q}{M_F} \cdot E(t) \quad (2.2)$$

Equation 2.1 explicitly uses  $\phi_i = \phi(X_i)$  where  $X_i = c R_i$  and  $c$  represents impurity concentration for each impurity site on a one dimensional line.  $R_i$  represents each place on a one dimensional line for each impurity site and is a randomly set, monotonically increasing function for each  $i^{\text{th}}$  index which grows larger . We also used a discretized second derivative<sup>9,10,11</sup>

$$\Delta^2 \phi_i = \frac{\phi_{i+1} - \phi_i}{X_{i+1} - X_i} - \frac{\phi_i - \phi_{i-1}}{X_i - X_{i-1}} \quad (2.3)$$

If we look at the first end point of the impurity sites , this procedure leads to a re-write of equation 2.3 which looks like<sup>12</sup>

$$\Delta^2 \phi_1 = \frac{\phi_2 - \phi_1}{X_2 - X_1} - \frac{\phi_1 - \phi_N}{X_1 - (X_N - L)} \quad (2.4)$$

where L is the grid length used in this simulation of CDW dynamics.

For the sake of including in both DC and AC contributions to an electric field, we can write

$$\mathbf{E} = \mathbf{E}_{\text{dc}} \quad (2.5)$$

and/or

$$\mathbf{E} = \mathbf{E}_{\text{dc}} + \mathbf{E}_{\text{ac}} \sin(\omega \tau) \quad (2.6)$$

When these electric field values are put into both Equation 2.1, we may then examine dielectric plots which are plotted against increasing frequency according to:

$$\text{Re } \varepsilon(\omega) = 4\pi \left( \frac{\text{Im } \sigma(\omega)}{\omega} \right) \quad (2.7)$$

and

$$\text{Im } \varepsilon(\omega) = 4\pi \left( \frac{\text{Re } \sigma(\omega)}{\omega} \right) \quad (2.8)$$

$$\text{Re } \sigma(\omega) \propto g1 \cdot \sum_n \left\langle \dot{\phi} \right\rangle_n \cdot \cos(\omega t_n) \cdot \Delta t \quad (2.9)$$

as well as

$$\text{Im } \sigma(\omega) \propto g1 \sum_n \left\langle \dot{\phi} \right\rangle_n \sin(\omega t_n) \cdot \Delta t \quad (2.10)$$

As written, the derivative of phase used here is from a second order Runge-Kutta simulation which was chosen for robustness of simulation . Having a higher order accurate simulation for the derivative of phase, as symbolically indicated above placed in what appears to be a first order calculation of conductivity would effectively negate the entire purpose of improved accuracy of taking the derivative of the phase calculation, as symbolically referred to in equation 2.1 . We must perform the DFT

inside the Runge-Kutta subroutine initially chosen to analyze the left hand side of equation 2.1. accurately. Otherwise, round off error from the first order conductivity calculation dominates , negating the second order calculations used for the current calculation. We find that if we re - scale dielectric measurements we re - scale dielectric measurements versus an applied electric field by resetting  $\epsilon / \epsilon_{initial}$  in place of just  $\epsilon$  versus E field (applied to an experimental sample ) that as the frequency  $\omega$  gets much smaller than  $\omega_c$  we observe increasingly non linear dielectric behavior as the E field approaches  $E_{th}$  . This is seen in **Figures 2a, 2b**

[ Place **Figure 2a, 2b** about here]

where we also define the critical frequency  $\omega_c$  value via a convention seen in **Figure 3**

[ Place **Figure 3** about here ]

### 3. **Review of the Q.M. numerical behavior of a single chain for CDW dynamics.**

Partly due to the failure of the classical model to avoid a blow up of the dielectric constant as discussed in the 2<sup>nd</sup> section of our presentation, we are then reviewing alternate computational models which could perhaps give us some of the numerical behavior which has more overlap with known experimental features as seen in previous device development lab ( TcSAM) experiments done in the 1990s up to 2000. In doing this we first examine. a quantum mechanical CDW model as introduced by Dr. Miller which answers certain physical issues well but which we found needed additional features built in

We are modifying a one chain model of Charge Density wave ( CDW ) transport initially pioneered by Dr. John Miller which furthered Dr. John Bardeens work on a



pinning gap presentation of CDW transport which involves a Hamiltonian modeling how CDW would move via modeling with S-S' pairs. The single chain model is a good way to introduce how a threshold electric field would initiate transport, qualitatively speaking. We did, however, when using it, assume that the charge density wave would be easily modeled with a soliton (anti-soliton) Gaussian packet, which is what we found needs further justification. So in lieu of this, we undertook this investigation to determine, among other things, necessary and sufficient condition to physically justify use of a soliton (anti-soliton) for our wave packet.

We start by using an extended Schwinger model<sup>3,13</sup> with the Hamiltonian set as

$$H = \int_x \left[ \frac{1}{2 \cdot D} \cdot \Pi_x^2 + \frac{1}{2} \cdot (\partial_x \phi_x)^2 + \frac{1}{2} \cdot \mu_E^2 \cdot (\phi_x - \varphi)^2 + \frac{1}{2} \cdot D \cdot \omega_p^2 \cdot (1 - \cos \phi) \right] \quad (3.1)$$

as well as working with a quantum mechanically based energy

$$E = i\hbar \frac{\partial}{\partial t} \quad (3.2a)$$

and momentum

$$\Pi = \left( \frac{\hbar}{i} \right) \cdot \frac{\partial}{\partial \phi} (x) \quad (3.2b)$$

The first case we are considering is a one-chain mode situation. Here, in order to introduce a time component,  $\Theta \equiv \omega_D t$  was used explicitly as a driving force, while using the following difference equation due to using the Crank Nickelson<sup>14</sup> scheme. We should note that  $\omega_D$  is a driving frequency to this physical system which we were free to experiment with in our simulations. The first index, j, is with regards to 'space', and the second, n, is with regards to 'time' step. Equation 3.3 is a numerical rendition of the

massive Schwinger model plus an interaction term, where one is calling  $E = i\hbar \frac{\partial}{\partial t}$  and

one is using the following replacement

$$\phi(j, n+1) = \phi(j, n-1) + i \cdot \Delta t \cdot \left( \frac{\hbar}{D} \left[ \frac{\phi(j+1, n) - \phi(j-1, n) - 2 \cdot \phi(j, n) + \phi(j+1, n+1) + \phi(j-1, n+1) - 2\phi(j, n+1)}{(\Delta x)^2} \right] - \frac{2 \cdot V(j, n)}{\hbar} \phi(j, n) \right) \quad (3.3)$$

We use these variants of Runge- Kutta in order to obtain a sufficiently large time step interval so as to be able to finish calculations in a reasonable period of time, while avoiding an observed spectacular blow up of simulated average phase values; one so bad that one gets nearly infinite wave function values after, say 100 time steps at  $\Delta t \approx 10^{-13}$ . Stable Runge- Kutta simulations require  $\Delta t \approx 10^{-19}$  Otherwise, one would need up to half a year on a PC in order to get the graph presented in **Figure 4** below :

[Put **figure 4** about here]

A second numerical scheme. the Dunford-Frankel and ‘fully implicit’<sup>14</sup> allows us to expand the time step even further. Then, the ‘massive Schwinger model’ equation has:

$$\phi(j, n+1) = \frac{2 \cdot \tilde{R}}{1 + 2 \cdot \tilde{R}} \cdot (\phi(j-1, n) - \phi(j+1, n)) + \frac{1 - 2 \cdot \tilde{R}}{1 + 2 \cdot \tilde{R}} \cdot \phi(j, n-1) \quad (3.4)$$

$$- i \cdot \Delta t \frac{V(j, n)}{\hbar} \phi(j, n)$$

where one has  $\tilde{R} = -i \cdot \Delta t \frac{\hbar}{2 \cdot D \cdot (\Delta x)^2}$ . The advantage of this model is that it is second

order accurate, explicit, and unconditionally stable, so as to avoid numerical blow up

behavior. One then gets resonance phenomena as represented by **Figure 4** given above.

This is to put it mildly quite unphysical and necessitates making changes, which we will be presenting in this manuscript.

#### **4. Addition of an additional term in the Massive Schwinger equation to permit formation of a soliton ( anti - soliton ) in our model.**

Initially we will present how addition of an interaction term between adjacent CDW chains will allow a soliton (anti – soliton) to form due to some analytical considerations we will present here. Then, we will show in a numerical simulation how these terms could lead to quantum tunneling. Finally we shall endeavor to show how our argument with the interaction term ties in with the fate of the false vacuum construction of soliton - anti soliton ( S-S' ) terms done in our prior publication where we used the Bogomil'nyi inequality <sup>2, 15</sup> as a necessary condition to the formation of S-S' term. Let us now first refer to how we can obtain a soliton via assuming that adjacent CDW terms can interact with each other.

There is an interesting interplay between the results of using the Bogomil'nyi inequality <sup>2, 15</sup> to obtain a S-S' pair which we approximate via a domain thin wall approximation <sup>2, 16</sup> and the nearest neighbor approximation of how neighboring chains inter-relate with one another to obtain a representation of phase evolution as an arctan function w.r.t. space and time variables. To wit, we can say that the Bogomil'nyi inequality provides for the necessity of a S-S' pair nucleating via a Gaussian approximation, while the interaction of neighboring chains of CDW material permits the existence of solitons (anti-solitons) in CDW transport.

The Bogomil'nyi inequality <sup>2,15</sup> permits the nucleation of a S-S' pair, whereas the 2<sup>nd</sup> argument we will bring up now is pertinent to if or not we may have the existence of an individual soliton (anti-soliton). This assumes we are using  $\Delta'$  as a Peierls gap <sup>17</sup> energy

term as an upper bound for energy coupling between adjacent CDW chains. Note that in the argument about the formation of a soliton (anti- soliton), that we use the following equation for a multi chain simulation Hamiltonian with Peierls condensation energy<sup>3,17</sup> used to couple adjacent chains (or transverse wave vectors):

$$H = \sum_n \left[ \frac{\Pi_n^2}{2 \cdot D_1} + E_1 [1 - \cos \phi_n] + E_2 (\phi_n - \Theta)^2 + \Delta' \cdot [1 - \cos(\phi_n - \phi_{n-1})] \right] \quad (4.1a)$$

with ‘momentum ‘ we define as

$$\Pi_n = \left( \frac{\hbar}{i} \right) \cdot \frac{\partial}{\partial \phi_n} \quad (4.1b)$$

We can reverse engineer this Hamiltonian to come up with an equation of motion which leads to a soliton, via use of taking the potential in equation 3.1a and then use a nearest neighbor approximation to use a Lagrangian based calculation of a chain of pendulums coupled by harmonic forces to obtain a differential equation which has a soliton solution. To do this, if we say that the nearest neighbors of the adjacent chains make the primary contribution, we may write the interaction term in the potential of this problem to be<sup>3</sup>

$$\Delta' (1 - \cos[\phi_n - \phi_{n-1}]) \rightarrow \frac{\Delta'}{2} \cdot [\phi_n - \phi_{n-1}]^2 + \text{very small H.O.T.s.} \quad (4.2)$$

and then considered a nearest neighbor interaction behavior via

$$V_{n.n.}(\phi) \approx E_1 [1 - \cos \phi_n] + E_2 (\phi_n - \Theta)^2 + \frac{\Delta'}{2} \cdot (\phi_n - \phi_{n-1})^2 \quad (4.3)$$

Here, we have that  $\Delta' \gg E_1 \gg E_2$  , so then we had a round off of

$$V_{n.n.}(\phi) \Big|_{\substack{\text{first} \\ \text{order} \\ \text{roundoff}}} \approx E_1 [1 - \cos \phi_n] + \frac{\Delta'}{2} \cdot (\phi_{n+1} - \phi_n)^2 \quad (4.4)$$

which then permits us to write

$$U \approx E_1 \cdot \sum_{l=0}^{n+1} [1 - \cos \phi_l] + \frac{\Delta'}{2} \cdot \sum_{l=0}^n (\phi_{l+1} - \phi_l)^2 \quad (4.5)$$

which allowed us, eventually, to obtain using  $L = T - U$  a differential equation of

$$\ddot{\phi}_i - \omega_0^2 [(\phi_{i+1} - \phi_i) - (\phi_i - \phi_{i-1})] + \omega_1^2 \sin \phi_i = 0 \quad (4.6)$$

with

$$\omega_0^2 = \frac{\Delta'}{m_e l^2} \quad (4.7)$$

and

$$\omega_1^2 = \frac{E_1}{m_e l^2} \quad (4.8)$$

where we assume the chain of pendulums, each of which is of length  $l$  actually will lead to a kinetic energy

$$T = \frac{1}{2} \cdot m_e l^2 \cdot \sum_{j=0}^{n+1} \dot{\phi}_j^2 \quad (4.9)$$

where we neglect the  $E_2$  value. However, as we state in our derivation of the formation of a S-S' pair, having  $E_2 \rightarrow \varepsilon^+ \approx 0^+$  would tend to lengthen the distance between a S-S' pair nucleating, with a tiny value of  $E_2 \rightarrow \varepsilon^+ \approx 0^+$  indicating that the distance  $L$  between constituents of a S-S' pair would get very large. We did, however, find that it was necessary to have a large  $\Delta'$  for helping us obtain a Sine-Gordon equation. This is so that if we set the horizontal distance of the pendulums to be  $d$ , then we have that the chain is of length  $L' = (n+1)d$ . Then, if mass density is  $\rho = m_e / d$  and we model this problem as a chain of pendulums coupled by harmonic forces, we set an imaginary bar with a quantity  $\eta$  as being the modulus of torsion of the imaginary bar, and  $\Delta' = \eta/d$ .

We have an invariant quantity, which we will designate as:  $\omega_0^2 d^2 = \frac{\eta}{\rho \cdot l^2} = v^2$ , which, as

$n$  approaches infinity, allows us to write a Sine - Gordon

$$\frac{\partial^2 \phi(x, t)}{\partial t^2} - v^2 \frac{\partial^2 \phi(x, t)}{\partial x^2} + \omega_1^2 \sin \phi(x, t) = 0 \quad (4.10)$$

with a way to obtain soliton solutions. In order to obtain soliton solutions, we introduce

dimensionless variables of the form  $z = \frac{\omega_1}{v} \cdot x$ ,  $\tau = \omega_1 \cdot t$ , leading to us finally obtain a

dimensionless Sine – Gordon equation we write as:

$$\frac{\partial^2 \phi(z, \tau)}{\partial \tau^2} - \frac{\partial^2 \phi(z, \tau)}{\partial z^2} + \sin \phi(z, \tau) = 0 \quad (4.11)$$

so that

$$\phi_{\pm}(z, \tau) = 4 \cdot \arctan \left( \exp \left\{ \pm \frac{z + \beta \cdot \tau}{\sqrt{1 - \beta^2}} \right\} \right) \quad (4.12)$$

where we can vary the value of  $\phi_{\pm}(z, \tau)$  between 0 to  $2 \cdot \pi$ , and here, below is an

example of how one can do just that: If one is looking at  $\phi_{+}(z, \tau)$  and set  $\beta = -.5$ , where

one has  $\tau = 0$  one can have  $\phi_{+}(z \ll 0, \tau = 0) \approx \varepsilon \approx 0$  and, also, have

$\phi_{+}(z = 0, \tau = 0) = \pi$ , whereas for sufficiently large  $z$  one can have  $\phi_{+}(z, \tau = 0) \rightarrow 2 \cdot \pi$ .

In a diagram with  $z$  as the abscissa and  $\phi_{+}(z, \tau)$  as the ordinate, this propagation of this

soliton ‘field’ from 0 to  $2 \cdot \pi$  propagates with increasing time in the positive  $z$  direction

and with a dimensionless ‘velocity’ of  $\beta$ . In terms of the original variables, one has that

the ‘soliton’ so modeled moves with velocity  $v \cdot \beta$  in either the positive or negative  $x$

direction. One gets a linkage with the original pendulum model linked together by

harmonic forces by allowing the pendulum chain as an infinitely long rubber belt whose

width is  $l$  and which is suspended vertically. What we have described is a flip over of a vertical strip of the belt from  $\phi = 0$  to  $\phi = 2 \cdot \pi$  which moves with a constant velocity along the rubber belt. This motion is typical of the soliton we have managed to model mathematically from our potential terms above. It is very important to keep in mind the approximations used above. First, we are using the nearest neighbor approximation to simplify equation 4.4. Then, we are assuming that the contribution to the potential due to the driving force  $E_2(\phi_n - \Theta)^2$  is a second order effect. All of this in its own way makes for an unusual physical picture, namely that the ‘capacitance’ effect given by  $E_2(\phi_n - \Theta)^2$  will not be a decisive influence in deforming the solution, and is a second order effect which is enough to influence the energy band structure the soliton will be tunneling through but is not enough to break up the soliton itself.

#### 4. Computer simulation work for multi chain representations of CDW transport

Now, our Peierls gap energy <sup>3,17</sup> was added to the massive Schwinger equation model <sup>13</sup> precisely due to the prior resonance behavior with a one chain computer simulation. We can now look at the situation with more than one chain. To do so, take a look at a Hamiltonian with Peierls condensation energy used to couple adjacent chains (or transverse wave vectors)<sup>3,18</sup>:

$$H = \sum_n \left[ \frac{\Pi_n^2}{2 \cdot D_1} + E_1 [1 - \cos \phi_n] + E_2 (\phi_n - \Theta)^2 + \Delta' \cdot [1 - \cos(\phi_n - \phi_{n-1})] \right] \quad (5.1)$$

and  $\Pi_n = \left( \frac{\hbar}{i} \right) \cdot \frac{\partial}{\partial \phi_n}$  and when we will use wave functions which are

$$\Psi = N \cdot \prod_j \left( a_1 \exp(-\alpha \cdot \phi_j^2) + a_2 \exp(-\alpha(\phi_j - 2 \cdot \pi)^2) \right) \quad (5.2)$$

with a two chain analogue of

$$\Psi_{two\ chains} = N \cdot \prod_{n=1}^2 \left( a_1 \exp(-\alpha \cdot \phi_j^2) + a_2 \exp(-\alpha(\phi_j - 2 \cdot \pi)^2) \right) \quad (5.2a)$$

If so, we put in the requirement of quantum degrees of freedom so that one has for each chain for a two dimensional case

$$|a_1|^2 + |a_2|^2 = 1 \quad (5.3)$$

which provides coupling between ‘nearest neighbor’ chains. In doing so, we are changing the background potential of this to a different situation where one has multiple soliton pairs that are due to the  $\Delta'$  term in which has huge cusps given which permit the existence of tunneling due to the band structure we will present as given in **Figure 5**, which we will describe in the next paragraph. We will first describe a two band structure and then generalize to a five band structure we will graph in **Figure 5** later on. First for a two cusp band situation with dynamical structure we have two chain interactions which we will describe here first. We should note that in tandem with NbSe<sub>3</sub> being quasi one

dimensional that  $\alpha \approx \frac{1}{\sqrt{\text{soliton width}}}$ . For ‘phase co-ordinate’  $\phi_j$ ,  $\exp(-\alpha \cdot \phi_j^2)$  is an

unrenormalized Gaussian representing a ‘soliton’ (anti – soliton) centered at  $\phi_j = 0$ , and

a probability of being centered there given by  $|a_1|^2$ . Similarly,  $\exp(-\alpha \cdot (\phi_j - 2 \cdot \pi)^2)$ . is

an un renormalized Gaussian representing a ‘soliton’(anti-soliton) centered at

$\phi_j = 2 \cdot \pi$  with a probability of occurrence at this position given by  $|a_2|^2$ . We can use

equation 5.3 to represent the total probability that one has some sort of tunneling

through a potential given by equation 5.1 dominated by the term  $\Delta'$  which dominates

the dynamics we can expect due to equation 5.1. We then are working with



$$E(\Theta) = \left\langle \Psi_{\text{two chains}} \left| H_{\text{two chains}} \right| \Psi_{\text{two chains}} \right\rangle \quad (5.4)$$

We observe a band structure of sorts given by this minimum ‘energy surface’ given in the graph of equation 5.4. And we find that the term  $\Delta'$  given in equation 4.4 is needed in order to get a band structure in the first place. The situation where we have a band structure with  $\Delta'(1 - \cos[\phi_2 - \phi_1])$  included<sup>3,18</sup> is, with Fortran 90, complicated since this would ordinarily imply coupled differential equations, which are extremely unreliable to solve numerically. For a number of reasons, one encounters horrendous round off errors with coupled differential equations solved numerically in Fortran. So, then the problem was done, instead, using Mathematica software which appears to avoid the truncation errors Fortran 90 presents us if we use a p.c. with standard techniques. Here is how the problem was presented before being coded for Mathematica: where one has  $E_1 = E_p = \text{pinning energy}$ ,  $E_2 = E_c = \text{charging energy}$ , and  $\Delta' \cdot [1 - \cos(\phi_2 - \phi_1)]$  represents coupling between “degrees of freedom” of the two chains. We for higher number of interacting chains generalize to  $\Delta' \cdot [1 - \cos(\phi_n - \phi_{n-1})]$ . When we have five interacting chains we have that the wave function used was set to a different value than given in either equations 5.2 or equation 5.2a

$$\Psi_m(\phi_i) = \sum_{m=-2}^2 b_m \exp(-\alpha(\phi_i - 2 \cdot \pi \cdot m)) \quad (5.5)$$

with:

$$\sum_{m=-2}^2 b_m^2 = 1 \quad (5.6)$$

we obtained a minimum energy ‘band structure’ with five adjacent parabolic arcs<sup>3,18</sup>. We obtain a ‘minimum’ energy out of this we can write as:

$$E = E_{\min} = \langle \Psi | \hat{H} | \Psi \rangle \quad (5.7)$$

where  $D_1 = 174.091, E_p = .00001, E_c = .000001$  and  $\Delta' = .005$  for Hamiltonian

$$\hat{H}_{two\ chains} = \sum_{n=1}^2 \left[ \frac{\Pi_n^2}{2 \cdot D_1} + E_1 [1 - \cos \phi_n] + E_2 (\phi_n - \Theta)^2 + \Delta' \cdot [1 - \cos(\phi_n - \phi_{n-1})] \right] \quad (5.8)$$

where minimum energy curves are set by the coefficients of the two wave functions, which are set as  $b_{-2}, b_{-1}, b_0, b_1, b_2; c_{-2}, c_{-1}, c_0, c_1, c_2; \alpha$  (which happens to be the wave parameter for equation 5.6). This leads to an energy curve given in **Figure 5**

[Put **Figure 5** about here]

where there are five local minimum potential energy values . It is a reasonable guess that for additional chains (i.e. if m bracketed by numbers  $> 2$ ) that the number of local minimum values will go up, provided that one uses a modified version of numerical simulation wave function as given in equation 5.5. We did the following to plot an average  $\langle \phi \rangle$  value, which we will represent in equation 5.10 below. The easiest way to put in a time dependence in the Hamiltonian (equation 5.8) is to provisionally set  $\Theta = \omega_D t$  for the graphics presented,  $\omega_D = 0.67$  M Hz

If we set  $\Psi \equiv \Psi(\phi_1, \phi_2, \Theta)$  which has an input from the Hamiltonian  $\hat{H}_{two\ chains}$

then we can set up an average phase, which we will call:

$$\Phi = \frac{1}{2}(\phi_1 + \phi_2) \quad (5.9)$$

where we calculate a mean value of phase given by <sup>3, 18</sup>

$$\langle \Phi(\Theta) \rangle = \int_{-\eta\pi}^{\eta\pi} \int_{-\eta\pi}^{\eta\pi} d\phi_1 d\phi_2 \frac{1}{2} \cdot (\phi_1 + \phi_2) |\Psi(\phi_1, \phi_2, \Theta)|^2 \quad (5.10)$$

The integral  $\langle \Phi(\Theta) \rangle$  was evaluated by ‘NIntegrate’ of Mathematica, and was graphed against  $\Theta$  in **Figure 6**, with  $\eta = 20$

[Put **Figure 6** about here]

. These total sets of graphs put together are strongly suggestive of tunneling when one has  $\Delta \neq 0$  in  $\hat{H}$  two chains .

The simulation results of **Figure 6** are akin to a thin wall approximation leading to a specific shape of the soliton – anti soliton pair in ‘phase’ space which is also akin to when we have abrupt but finite transitions after long periods of stability <sup>1,2</sup> . We can link this sort of abrupt transitions to what happens when we have a ‘thin wall approximation’ as spoken of by Sidney Coleman in his ‘fate of the false vacuum’ hypothesis <sup>4</sup> for ‘instanton’ transitions. We do, however, need to verify if or not that the soliton solution to this problem is optimal for tunneling. Trying to show this will be the main reason for the next section treatment of how a multi chain interaction will be a necessary condition for formation of solitons ( anti- solitons) in CDW transport problems. This is when we will be working with wave functionals of the form given by initial and final wave functionals looking like

$$\begin{aligned} \Psi_i[\phi(x)]_{\phi=\phi_{ci}} &= c_i \cdot \exp\left\{-\alpha \cdot \int dx [\phi_{ci}(x) - \phi_0(x)]^2\right\} \\ \Psi_f[\phi(x)]_{\phi=\phi_{cf}} &= c_f \cdot \exp\left\{-\alpha \int dx [\phi_{cf}(x) - \phi_0(x)]^2\right\} \end{aligned} \quad (5.11a,b)$$

## 6: **Conclusion: Setting up the framework for a Field Theoretical Treatment of Tunneling.**

We have, in the above identified pertinent issues needed to be addressed in an analytical treatment of Charge Density Wave transport. First, we should try to have a formulation of the problem of tunneling which has some congruence with respect to the ‘False Vacuum’ hypothesis of Sidney Coleman. We make this statement based upon the abrupt transitions made in a multi chain model of Charge Density Wave tunneling which are in form identical to what we would expect in a thin wall approximation of a boundary between true and false vacuums. Secondly, we also can say that it is useful to keep a soliton (anti - soliton) representation of solutions for Charge Density transport. **Figure 5** and **Figure 6** address minimum conditions for the formation of a soliton (anti-soliton), but what we have here is that if we want to have a band structure pertinent to tunneling analysis, we should keep the  $\Delta'$  term necessitated in coupling chains together in Charge Density Wave transport analysis.

We explicitly argue that a tunneling Hamiltonian based upon functional integral methods is essential for satisfying necessary conditions for the formation of a S-S' pair. The Bogomil'nyi inequality stresses the importance of the relative unimportance of the driving force  $E_2 \cdot (\phi_n - \Theta)^2$ , which we drop out in our formation of a soliton (anti soliton) in our multi chain calculation. In addition, we argue those normalization procedures, plus assuming a net average value of the  $\Delta'(1 - \cos[\phi_n - \phi_{n-1}]) \rightarrow \frac{\Delta'}{2} \cdot [\phi_n - \phi_{n-1}]^2 + \text{small terms}$  as seen in our analysis of the contribution to the Peierls gap contribution to S-S' pair formation in our Gaussian<sup>1,2</sup> wave functional equations 5.11a,b where the normalizing term  $c_{i,f}$  would allow us to scale out an averaged out value of the

$\Delta'(1 - \cos[\phi_n - \phi_{n-1}]) \rightarrow \frac{\Delta'}{2} \cdot [\phi_n - \phi_{n-1}]^2$  representation of how S-S' pairs interact in a multi chain model evolve in a pinning gap transport problem for charge density wave dynamics. This would allow us, if done, to have S-S' pairs being used in equation 5.13 due to their formation in our problem due to the Peierls gap term in the Hamiltonian<sup>3,18</sup>. Then the fate of the false vacuum hypothesis used<sup>1,2,3</sup> so that the S-S' pairs can have nucleation behavior as seen in **Figure 7**

[ place **Figure 7** about here ]

is consistent with a Gaussian wave functional representation of transport behavior<sup>1,2</sup> leading to matching with experimentally observed current behavior<sup>2,3</sup> as seen in **Figure 8** below. This would permit us to form necessary and sufficient conditions for permitting a Gaussian wave functional to use S-S' pairs to form the current experimentally observed in **Figure 8** below, where after a long derivation<sup>1,2,3</sup> we have

[ place **Figure 8** about here ]

where we write

$$I \propto \tilde{C}_1 \cdot \left[ \cosh \left[ \sqrt{\frac{2 \cdot E}{E_T \cdot c_V}} - \sqrt{\frac{E_T \cdot c_V}{E}} \right] \right] \cdot \exp \left( \frac{-E_T \cdot c_V}{E} \right) \quad (6.1)$$

$$\text{with } \tilde{C}_1 \equiv \frac{C_1 \cdot C_2}{2 \cdot m^*}$$

which is a significant improvement over a prior expression derived to qualitatively fit experimental data<sup>19</sup>

$$I \propto G_p \cdot (E - E_T) \cdot \exp \left( \frac{-E_T}{E} \right) \quad \text{if } E > E_T \quad (6.2)$$

$$0 \quad \text{otherwise}$$

### Figure Captions

**FIG 1** Average phase  $\langle\phi\rangle$  plotted against time (for  $E_{dc}$ ) with  $\langle\phi\rangle$  stabilizing if  $E_{dc} < E_{th}$  and  $\langle\phi\rangle$  monotonically increasing if  $E_{dc} > E_{th}$ .

**FIG 2** Comparison of scaled dielectric values when one has signal frequency  $\omega \leq \omega_c$  i.e. near a critical value  $\omega_c$ . Figure 2a is for low frequency plots, and figure 2b is high frequency plots. One obtains the situation that there is a blow up of the dielectric response if one has the electric field exceeding a threshold value, which could not be duplicated numerically. The dielectric is infinite valued when  $E=E_{th}$

**FIG 3** This conductivity plot shows the origins of how we pick critical value  $\omega_c$

**FIG 4:** Beginning of resonance phenomena in single chain quantum dynamics due to using the traditional Crank – Nickelson numerical iteration scheme of the one chain model.

**FIG 5:** Determining band structure via a Mathematica 8 program, and with wave functions given by equation 4.6,

**FIG 6:** Phase vs.  $\Theta$ , according to the predictions of the ‘multi- chain’-tunneling tunneling model.

**FIG 7:** Evolution from an initial state  $\phi_i$  to a final state  $\phi_f$  for a double-well potential (inset) in a 1-D model, showing a kink-antikink pair bounding the nucleated bubble of true vacuum. The shading illustrates quantum fluctuations about the classically optimum

configurations of the field  $\phi_i(x) = 0$  and  $\phi_f(x)$ , while  $\phi_0(x)$  represents an intermediate field configuration inside the tunnel barrier

**FIG 8** : Experimental and theoretical predictions of current values. The dots represent a Zenier curve fitting polynomial, whereas the blue circles are for the S-S' transport expression derived with a field theoretic version of a tunneling Hamiltonian.

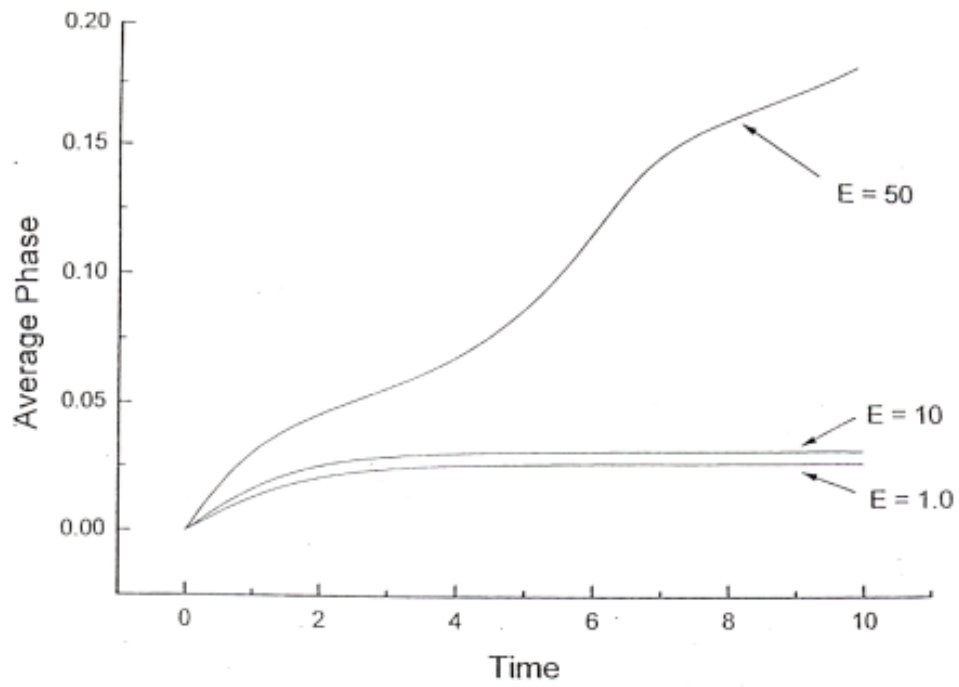


**Fig 1**

**Beckwith**



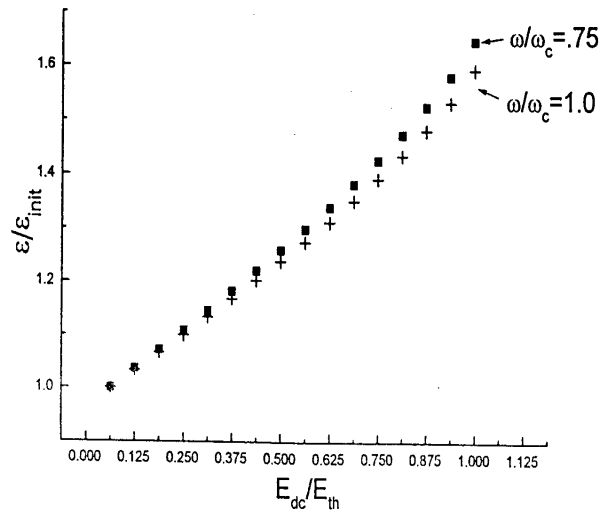


Figure 2a

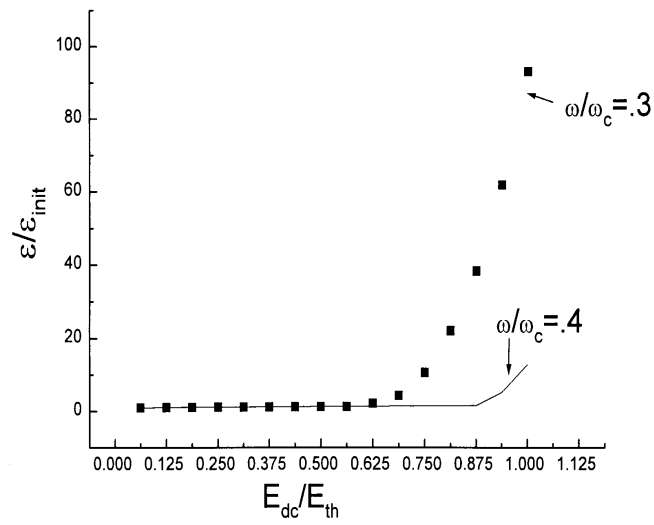
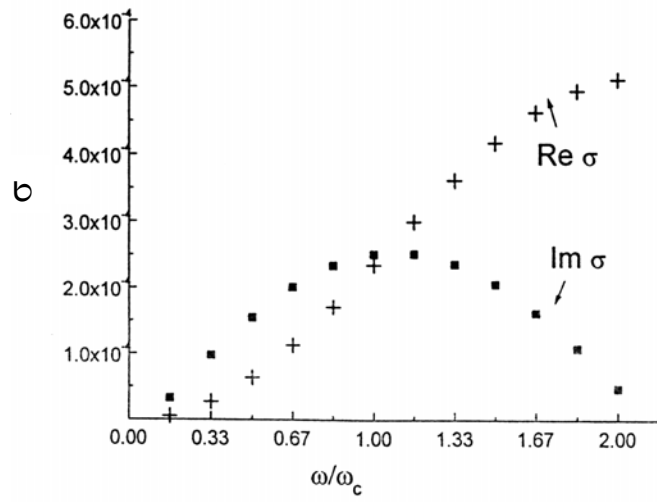


Figure 2b

Beckwith



**Figure 3**

**Beckwith**

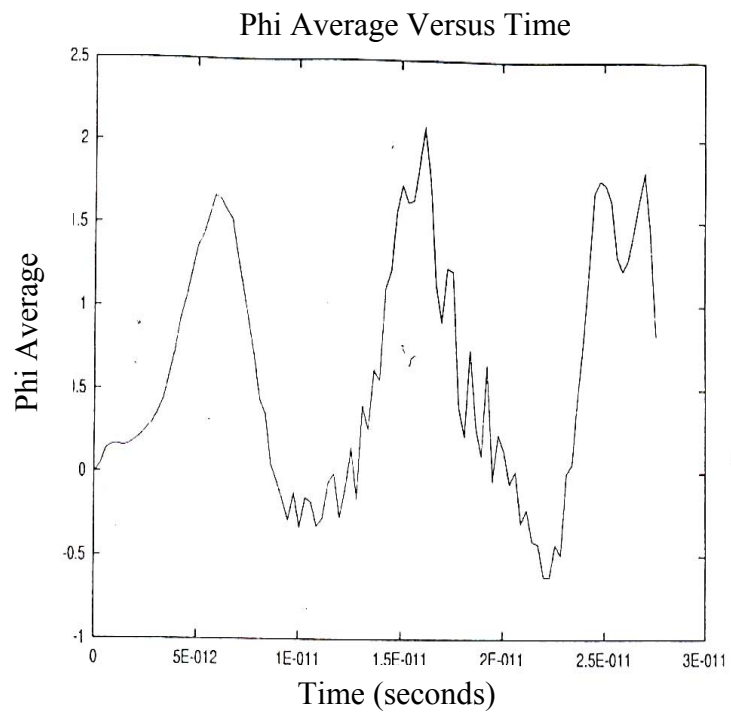


**Figure 4**

**Beckwith**

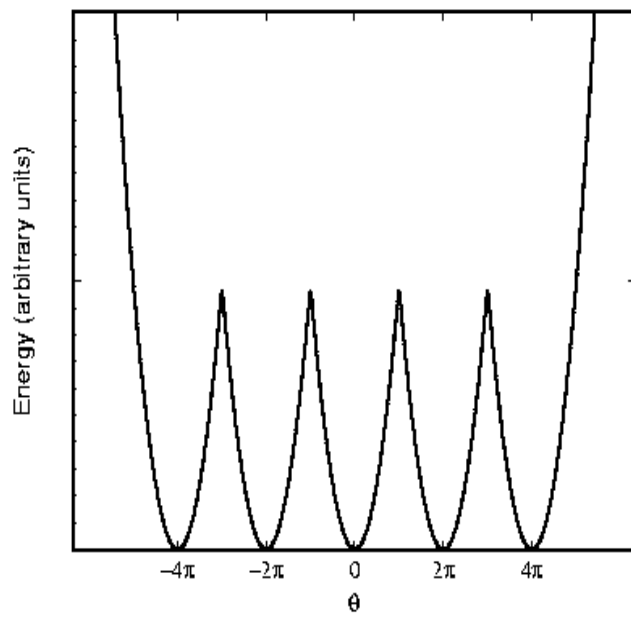


**Figure 5**

**Beckwith**

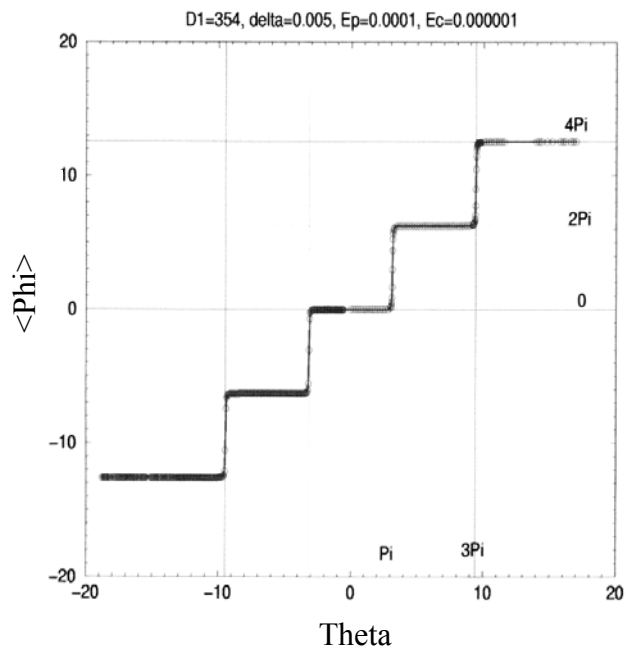


**Figure 6**

**Beckwith**

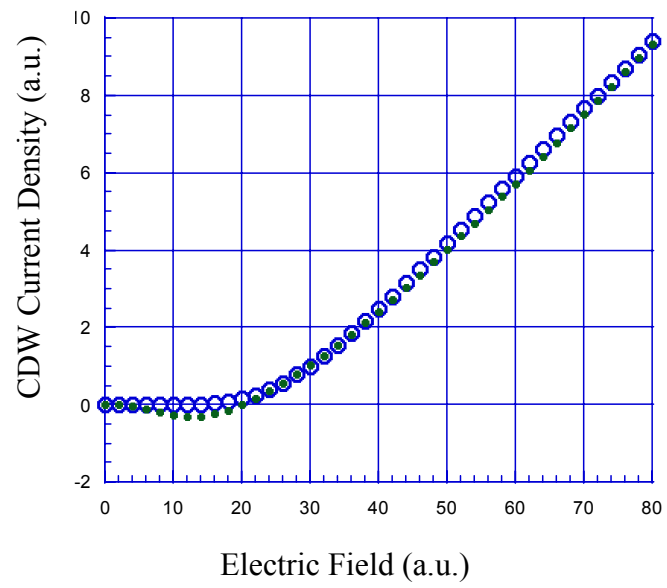


**Figure 7**

**Beckwith**

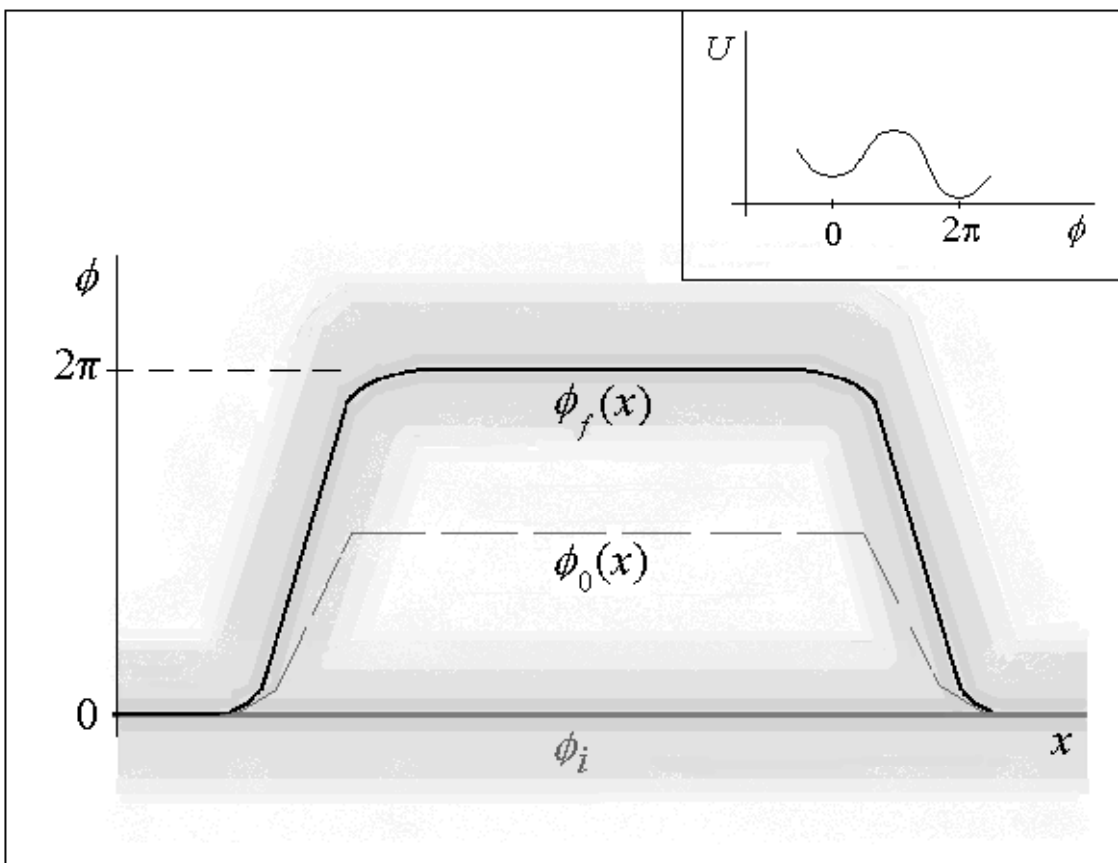


Figure 8

Beckwith

## References

---

- <sup>1</sup> A. W. Beckwith, J.H. Miller, Jr, arxiv : math-ph/0406048 (Tunneling Hamiltonian Representation of False Vacuum Decay I .Comparison with Bogomol'nyi Inequality ; A.W. Beckwith, J.H. Miller)
  
- <sup>2</sup> A.W. Beckwith , J.H. Miller, jr ; arxiv : math-ph/0406053 (Tunneling Hamiltonian Representation of False Vacuum Decay II. Application to Soliton – Anti Soliton Pair Creation ; A.W. Beckwith, J.H. Miller)
  
- <sup>3</sup> A.W. Beckwith ‘Classical and Quantum models of Density wave transport: A comparative study’ PhD dissertation , U. of Houston physics department , December 2001
  
- <sup>4</sup> S. Coleman , Phys. Rev. D 15,2929(1977)
  
- <sup>5</sup> P.B Littlewood, Phys. Rev B 33, 6694 (1986)
  
- <sup>6</sup> H. Fukuyama and P.A. Lee , Phys. Rev B 17, 535 (1977)
  
- <sup>7</sup> P. A. Lee and T.M. Rice, Phys. Rev B 19,3970 (1979)
  
- <sup>8</sup> S. Kagoshima, H. Nagasawa, T. Sambongi ‘ One dimensional Conductors’, Springer – Verlag, 1987, pp 32-34, in particular equation 2.74
  
- <sup>9</sup> P.B Littlewood, Phys. Rev B 33, 6694 (1986), see equation 2.5
  
- <sup>10</sup> P.B Littlewood, Phys. Rev B 33, 6694 (1986), see equation 2.6
  
- <sup>11</sup> L. Pietronero and S. Strassler, Phys. Rev B 28, 5863 (1983); H. Matsukawa and H. Takayama, Solid State Commun. 50, 283(1984)
  
- <sup>12</sup> Private communications with Dr. Bill Mayes II
  
- <sup>13</sup> J. H. Miller, Jr. , C. Ordonez, and E. Prodan, Phys. Rev. Lett 84, 1555(2000)
  
- <sup>14</sup> G. Smith, ‘ Numerical Solutions of Partial Differential equations; Finite difference Methods’ , third edition, Oxford, 1986 ; K. Morton Morton and D. Mayers; ‘ Numerical Solution of Partial Differential equations: An introduction’
  
- <sup>15</sup> A. Zee, ‘ Quantum field theory in a nutshell’ ; Princeton university press , 2003 pp. 279-80



---

<sup>16</sup> J. H. Miller, Jr., G. Cardenas, A. Garcia-Perez, W. More, and A. W. Beckwith, J. Phys. A: Math. Gen. 36, 9209 (2003).

<sup>17</sup> S. Kagoshima, H. Nagaswawa, T. Sambongi, 'One dimensional conductors', Springer Verlag 1987

<sup>18</sup> J. H. Miller, Jr., G. Cardenas, A. Garcia-Perez, W. More, and A. W. Beckwith, J. Phys. A: Math. Gen. 36, 9209 (2003).

<sup>19</sup> J.H. Miller, J. Richards, R.E. Thorne, W.G. Lyons and J.R. Tucker ; Phys.Rev. Lett. 55,1006 (1985)